Geografia-Malaysian Journal of Society and Space 20 issue 1 (99-120)
 https://doi.org/10.17576/geo-2024-2001-07

Impacts of urban land use and land cover changes on land surface temperature in Kuala Lumpur, Malaysia

Nur Hakimah Asnawi[1], Lam Kuok Choy[1*], Rosniza Aznie Che Rose[1], Millary Agung Widiawaty[2,3,4], Moh. Dede[5,6], Farah Nuralissa Muhammad[1]

[1]Geography Programme, Center for Research in Development, Social and Environment, Faculty of Social Science and Humanity, Universiti Kebangsaan Malaysia, 43600 UKM Bangi, Selangor, Malaysia
[2]Cakrabuana Institute for Geoinformation, Environment and Social Studies (CIGESS), Ciledug, Cirebon Regency, West Java 45188, Indonesia
[3]Directorate for Development Policy, National Research and Innovation Agency of Indonesia (BRIN), Jakarta Pusat, DKI Jakarta 10340, Indonesia
[4]School of Geography, Earth and Environmental Sciences, University of Birmingham, Edgbaston, Birmingham B15-2TT, United Kingdom
[5]Doctoral Program on Environmental Science, Postgraduate School (SPS), Universitas Padjadjaran, Bandung City, West Java 40132, Indonesia
[6]Faculty of Social Sciences Education, Universitas Pendidikan Indonesia, Bandung City, West Java 40154, Indonesia

Correspondence: Lam Kuok Choy (email: lam@ukm.edu.my)

Received: 30 September 2023; Accepted: 5 February 2024; Published: 29 February 2024

Abstract

Urbanisation has triggered massive development activities which led to significant changes in land use and land cover (LULC). Fundamentally, the changes in LULC has to be monitored to detect the presence of regional environmental changes and impacts. Hence, this study aims to evaluate the effects of LULC changes on land surface temperature (LST) in Kuala Lumpur from 1990 to 2022 using remote sensing data. The time-series Landsat data was used to map the LULC changes, and the LST was retrieved from the Landsat thermal bands. Normalised Difference Vegetation Index (NDVI) was computed to determine its relationship with LST and LULC. The findings show more than 68% of vegetation cover in Kuala Lumpur vanished within 32 years, while the built-up land expanded by more than 50%, and water bodies dropped by more than 45%. The correlation between LST and NDVI is associated with the distribution of vegetation cover, where LST is inversely related to NDVI. A decrease in the NDVI mean value from 0.3 to 0.2 in 2022 reflected in the rise of an average mean of LST from 22.9°C to 26.2°C in 2022. A decrease in vegetation cover can contribute to the increase in surface temperature. Hence, it can be inferred that it is essential to take effective approaches in urban development planning to minimise effects on urban climate change.

Keywords: LST, NDVI, remote sensing, satellite imagery, urban LULC

Introduction

Over the last few decades, the growth of the global population boosted urbanisation triggering massive development all over the world. The United Nations (2019) reported that urban population increased from 30% in 1950 to 55% in 2018 with more world population residing

in urban areas compared to rural areas since 2007. Population growth acts as a catalyst in regional development as it encourages urbanisation which in turn promote better economic growth and human development. However, unplanned urbanisation could lead to environmental degradation and sustainability impairment (Rahman et al., 2011). Land use and land cover (LULC) are most affected by accelerated anthropogenic activities due to urbanisation (Alawamy et al., 2020), particularly in the transformation of green space to urban construction on a large scale with a significant impact on the ecosystem (Al-sharif & Pradhan, 2014). Geist and McConnell (2006) pointed out that the biophysical, economic, and technological, demographic, institutional and cultural factors influence the LULC changes.

The LULC changes have been universally recognised as crucial aspects leading to changes in global biodiversity and ecosystems due to their significant impacts (Angessa et al., 2019; Aspinall, 2008). The rising temperature of the surface due to the transformation of green cover into impermeable surfaces are perceived as one of the most concerning impact of LULC changes in urban areas (Mallick et al., 2008) which in turn triggers the urban heat island phenomenon (Pamungkas et al., 2019; Weng et al., 2004; Quattrochi & Luvall, 1999). These alterations affect the solar radiation absorption, surface temperature, heat storage, rates of evaporation and wind turbulence in the cities (Mallick et al., 2008). Having said that, unplanned urban growth with high urban density and less vegetation cover can largely impact the thermal behaviour of urban areas (Bek et al., 2018). To acquire an advance understanding of the thermal behaviour, the land surface temperature (LST) can be recorded to deliver essential information on the characteristics of the physical surface climate. Generally, LST can be simply defined as the radiative skin temperature of any surface (Kumar & Shekhar, 2015) that can be measured (Jeevalakshmi et al., 2017a). LST involves the measurement of thermal infrared radiation emission which is known as radiometric temperature (Mohd Jaafar et al., 2020).

Besides anthropogenic activities, global climate change is likely to affect LST through the El Nino and La Nina phenomena that are believed to be the main determinant of fluctuating LST (Yan et al., 2020). The changes in LST crucially affect socioeconomic which contributed to human thermal displeasure and threatens the living, particularly during warm seasons (Mashhoodi, 2021). In addition, LST would affect the environment and ecosystem, mainly in saturated urban areas (Imran et al., 2021) as well as influence the regional energy balance (Islam & Ma, 2018). Subsequently, it could be one of the sources of the formation of the urban heat island phenomenon due to intensive land surface changes (Tang et al., 2017). Therefore, it is essential to understand the LST conception and its relationship with other variables for urban planning and management.

There are many published studies (Dede et al., 2019; Pal & Ziaul, 2017; Tran et al., 2017; Sahana et al., 2016; Zhou & Wang, 2011; Jiang & Tian, 2010) which described the relationship between LULC changes and LST. Some even revealed that the rapid LULC changes influenced the thermal behaviour because a high rate of urbanisation can accelerate the LST concentration in urban areas (Hua & Ping, 2018; Fu & Weng, 2016; Sahana et al., 2016; Qian et al., 2006). A similar pattern was also noticed within the urban areas of Malaysia (Tan et al., 2010; Tan et al, 2009). Particularly, the Klang Valley region experienced the most significant LULC changes which affected the regional LST or urban climate (Buyadi et al., 2014; Tehrany et al., 2013; Takeuchi et al., 2010). This scenario occurred because of the replacement of natural land cover by non-evaporating surfaces that contributed to the increasing surface temperature and the atmosphere above (Hua & Ping, 2018; Amanollahi et al., 2016). Therefore, preserving and conserving the green cover in the urban environment is essential in combating the negative consequences of climate change (Sheikhi et al., 2015).

Accordingly, remote sensing is an influential tool in monitoring and quantifying the urban built-up area growth and evaluating its impacts on regional climate (Anasuya et al., 2019). Various acquisition platforms of LST retrieval, such as satellite, airborne and unmanned

aerial vehicle (UAV) based thermal infrared (TIR) sensors are available to monitor the impacts of urbanisation on LST (Fu & Weng, 2016). Among the various available thermal infrared sensors to derive LST include Advanced Very High-Resolution Radiometer (AVHRR), Terra-Advanced Spaceborne Thermal Emission and Reflection Radiometer (ASTER), Moderate Resolution Imaging Spectroradiometer (MODIS), Geostationary Operational Environmental Satellite (GOES), Enhanced Thematic Mapper Plus (ETM+), Thematic Mapper (TM) and Thermal Infrared Scanner (TIRS) (Li et al., 2013; Coll et al., 2012; Coll et al., 2010; Mallick et al., 2008). To date, time-series data from these sensors have been widely performed at regional to global scales.

This study aims to integrate remote sensing data and Geographic Information System (GIS) application in identifying probable modifications of LST because of the changes of LULC in Kuala Lumpur within 32 years between 1990, 2015 and 2022. Meanwhile, the LULC and Normalised Difference Vegetation Index (NDVI) were utilised as indicators to measure their influences on LST. As one of the fastest-growing cities in Asia, the Federal Territory of Kuala Lumpur has experienced an extensive urban development that enthralling for further study. Thus, this research findings might be contributed to providing extra research resources and essential insights into the complex interaction between varied variables of urban settings and its environmental changes.

Study area

This research was conducted in Kuala Lumpur, the capital city of Malaysia which lies at 3° 8’ N, 101° 41’ E, (Figure 1). Kuala Lumpur located in the middle of Selangor state was once a territory of Selangor before being separated from the state in 1974 to structure the Federal Territory which is now governed by the Malaysian Federal Government. The Kuala Lumpur City Hall (DBKL) is its local authority responsible for the administration and management of the city. Kuala Lumpur is composed of 243 km^2 total area, wider flat topography with an average elevation of 81.95 m and has a total population of 1.79 million as of 2018. As Malaysia is a tropical country located near the equator, Kuala Lumpur’s climate is hot and humid throughout the year with a temperature range of 28-32 °C and received an annual average of 110 mm precipitation intensity. Kuala Lumpur comprises eleven districts including Kepong, Batu, Wangsa Maju, Setiawangsa, Titiwangsa, Segambut, Bukit Bintang, Lembah Pantai, Seputeh, Cheras and Bandar Tun Razak. As the most urbanised city of the country located within the Klang Valley, Kuala Lumpur is an economic and business hub which has witnessed rapid urban development and became the fastest-growing region in Malaysia. Thus, more than 80 % of Kuala Lumpur to date are being covered by built-up land use categories such as residential, commercial, industrial, institutional, and other uses.

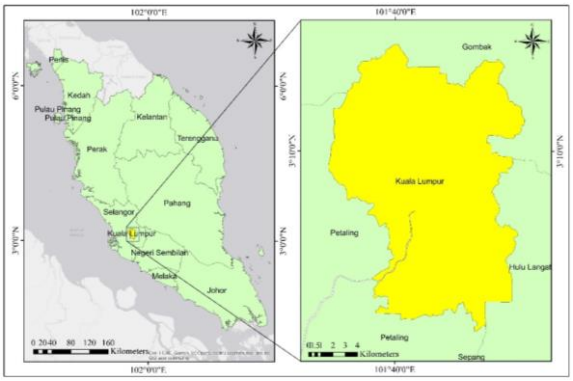

Figure 1. The location map of Kuala Lumpur, Malaysia

Materials and methods

The methodological framework adopted in this study involved different analytical processes of Landsat imagery to examine the effects of the LULC changes on land surface temperature. Figure 2 showed the study processes involved which include (1) data collection and preprocessing; (2) classification and post-classification of satellite images; (3) accuracy assessment; (4) NDVI value derivation; (5) retrieval of LST and (6) the interpretation of LULC, NDVI and LST interactions.

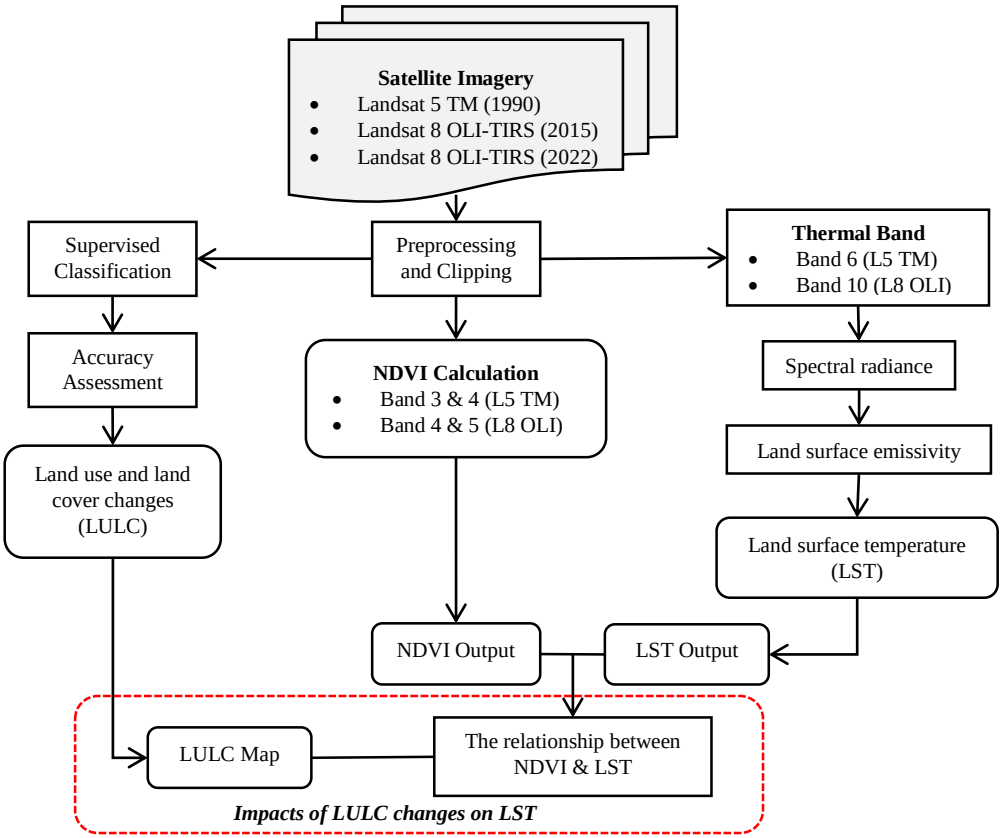

Figure 2. The methodological framework applied in analysing the impact of LULC changes on LST by using Landsat images of Kuala Lumpur for 1990, 2015 and 2022

Satellite images and data pre-processing

Satellite images for 1990 from Landsat 5 Thematic Mapper (TM) and Landsat 8 Operational Land Imager and Thermal Infrared Sensor (OLI-TIRS) for 2015 and 2022 were obtain from the United States Geological Survey (USGS) archive and were used to analyse the changes in LULC in Kuala Lumpur. All the images were selected based on the clarity of the images with less cloud coverage, moreover, the images were all captured in the month of May for the corresponding years. Multispectral Landsat imagery provided a 30 meters spectral resolution aiding in image interpretation and increased accuracy of the study. The selected images also had an existing WGS_1984_UTM_Zone_47N projection system. The acquired satellite images were then converted from Digital Number (DN) into reflectance to produce the units of physical interpretation and quantitative value so that the spectral signature on the Earth's surface is readable. Next, the images were clipped according to the required boundary to segregate the study area to facilitate the image processing work and reduce redundant data.

Image classification and post classification

The multispectral images with the best band combination were formed to differentiate the variations in brightness and visual quality of the images according to several land use categories. The band composition of 4-5-3 for Landsat 5 and band composition of 5-6-4 for Landsat 8 images were adopted to visualise the images for land use classification. Furthermore, a supervised classification technique was applied to produce a LULC map in this study. Supervised classification requires the use of training area data that is considered representative of each land type or surficial unit to be classified (Killeen et al., 2015). The identified three main land use categories in study area included vegetation cover, built-up area, and water bodies. The popular supervised classification algorithm of maximum likelihood was applied where all pixels were assigned into the land use class with the highest probability.

Accuracy assessment

Accuracy assessment was carried out following the land-use classification process to calculate the validation rate of image classification was true according to the ground truth. The accuracy task was attained based on the error matrix table between classified images with the actual ground truth data to determine the Cohen's Kappa coefficient value. Kappa coefficient is the calculation for accuracy assessment developed by Cohen (1960) as indicated in Equation [1]. The error matrix and Kappa coefficient applied in various land classification studies are a standard means of accuracy assessment for image classification (Rwanga & Ndambuki, 2017).

$$\mathrm{k} = \frac{\mathrm{observed}-\mathrm{expected}}{1-\mathrm{expected}} \quad [1]$$

Normalized Difference Vegetation Index (NDVI)

NDVI indicates the estimation of green cover density (Weier & Herring, 2000). NDVI is computed based on near-infrared (NIR) and red (RED) light reflectance assessment as indicated in Equation [2].

$$\mathrm{NDVI} = \frac{(\mathrm{NIR}-\mathrm{RED})}{(\mathrm{NIR}+\mathrm{RED})} \quad [2]$$

In this study, the Landsat 5 TM image with calibrated band 3 and 4 and Landsat 8 OLI-TIRS with calibrated band 4 and 5 were utilised to derive the NDVI value based on the Equation [2]. The values of NDVI fall within the range of -1 to 1, whereby a positive value indicates highly green cover, whilst the density of green cover is lower with a negative value.

Land Surface Temperature (LST) extraction

The extraction of LST was performed by processing the thermal bands of Landsat images using the mono-window algorithm initiated by Qin et al. (2001). As for Landsat 5 TM, the thermal band was band 6 (10.40 – 12.50 µm), while band 10 (10.60 – 11.19 µm) and band 11 (11.50 – 12.51 µm) were the thermal bands for Landsat 8 TIRS imagery. For the LST extraction of Landsat 8 data, Montanaro et al. (2014) recommended the utilisation of band 10 over band 11, as band 10 receives less stray light effects and demonstrates sufficient performance compared to band 11. Therefore, band 10 was utilised in this study only for the LST extraction of 2015 and 2022. Moreover, the few steps to derive LST from Landsat TM and OLI consisted of the

DN conversion into spectral radiance and then spectral radiance converted to brightness temperature that could be calculated based on Equation [3] until Equation [7] that were adopted and adapted from Jeevalakshmi et al. (2017b), Wang et al. (2015), and Zhibin et al. (2015). The transformation of DN into radiance was derived by Equation [3]:

$$L_\lambda = M_\iota * QCAL + A_\iota \quad [3]$$

where

L_λ = the spectral radiance of thermal band ($w \cdot sr^{-1} \cdot m^{-3}$)
M_ι = the slope of the radiance/DN conversion function
QCAL = the DN value of pixel, which, Landsat 5 = Band 6 image; Landsat 8 = Band 10 image
A_ι = the intercept of the radiance/DN conversion

Meanwhile, the conversion of the spectral radiance to brightness temperature is represented by Equation [4]:

$$T_B = \frac{K_2}{\ln(1 + \frac{K_1}{L_\lambda})} - 273.15 \quad [4]$$

where

T_B = Brightness temperature in degree Celsius (°C)
K_1 = Calibration constant 1, which (Landsat 5 = 607.76; Landsat 8 = 774.89)
K_2 = Calibration constant 2, which (Landsat 5 = 1260.56; Landsat 8 = 1321.08)
L_λ = Result of Equation [3]
.

Finally, the LST value was computed using Equation [5]:

$$LST = \frac{T_B}{1 + [\left(\lambda * \frac{T_B}{\rho}\right) * \ln \varepsilon]} \quad [5]$$

where

LST = Land surface temperature in degree Celsius (°C)
T_B = Brightness temperature
λ = the effective wavelength (Landsat 5 = 11.5 µm; Landsat 8 = 10.9 µm)
ρ = $h \times c/\sigma$ (1.438×10^{-2} mK);
where h is the Plank's constant (6.626×10^{-34}), c is the light velocity (3×10^8 m/s) and σ is the Boltzmann constant (1.38×10^{-23}).
ε = Emissivity of land surface

The land surface emissivity (LSE) is derived from Equation [6]:

$$\varepsilon = 0.004 * P_v + 0.986 \quad [6]$$

where

ε = LSE
P_v = Proportion of vegetation

From Equation [6], the proportion of vegetation was computed based on Equation [7]:

$$P_v = \left(\frac{NDVI_{jr} - NDVI_{min}}{NDVI_{max} - NDVI_{min}}\right)^2 \quad [7]$$

where

$NDVI_{jr}$ = Result of Equation [2]
$NDVI_{max}$ = 0.5
$NDVI_{min}$ = 0.2

Sobrino et al. (2004), Sobrino and Raissouni (2000) suggested using the minimum and maximum values of the NDVI image of 0.2 and 0.5 respectively that represented the values for soil pixel (min) and vegetation pixel (max) for global scale applications.

Results

Accuracy assessment

Accuracy assessment is necessary for processing the remote sensing data. In this study, the imagery from Google Earth was utilised as a reference source to the classified LULC map of 1990, 2015 and 2022 to validate the classified images. The same set of generated random points by random sampling method was used on the classified image and Google Earth for three study years. Table 1 summarises the accuracy assessment results yielded from the error matrix and Kappa analysis. The user's accuracy refers to the commission errors related to the classified map result, while the producer's accuracy indicated the error of omission for the reference data. The classified LULC map of 1990 yielded 91% of overall accuracy with 0.83 Kappa agreement. On the contrary, the accuracy assessment of the classified LULC map of 2015 yielded 65% overall accuracy with a Kappa agreement of 0.74. Meanwhile, the 2022 classified LULC map produced 88% of overall accuracy with Kappa agreement of 0.75. These Kappa coefficient results indicated that the classified images were relevant for further research. Based on the result, the accuracy of 2015 was much lower than that of 1990 and 2022because of the noisy data with more cloud and shadow existence in the 2015 satellite image. Thus, some random points were required to be excluded in accuracy computation. Besides, the fragmentation of vegetation in 2015 became greater with many smaller vegetation polygons scattered around due to rapid development which could affect the accuracy because of the relatively rough pixel size of 30m Landsat.

Table 1. Accuracy assessment of LULC of Kuala Lumpur in 1990, 2015 and 2022

Category	Classification accuracy					
	1990		2015		2022	
	User's accuracy (%)	Producer's accuracy (%)	User's accuracy (%)	Producer's accuracy (%)	User's accuracy (%)	Producer's accuracy (%)
Vegetation	84	95	95	61	92	75
Water bodies	100	100	100	75	100	60
Built-up	97	89	88	100	85	97
Overall Accuracy	**91%**		**65%**		**88%**	
Kappa	**0.83**		**0.74**		**0.75**	

Land use and land cover (LULC) analysis

Table 2 illustrates the summary statistics of the LULC changes in 1990, 2015 and 2022 in Kuala Lumpur. There was a significant reduction in vegetation area from 10,212 hectares to 2,779 hectares, approximately 70% of area depreciation within 25 years from 1990 to 2015. However, there was a marginally increase of 457 hectares of vegetation area by 2022 compared to previous year. On the other hand, built-up areas increased significantly by 54.53% from 13,737 hectares to 21,228 hectares between 1990 and 2015. Nonetheless, the built-up areas in 2022 slightly loss 327 hectares of its area. Meanwhile, the water bodies category decreased by 28.37% from 416 hectares in 1990 to 298 hectares in 2015 and continuously deteriorated by 2022 with only 228 hectares remaining. The statistics of land-use changes revealed that more than 85% of Kuala Lumpur's total land area is now dominantly consisted of built-up area, then vegetation and water bodies.

Table 2. Land use and land cover statistics in Kuala Lumpur for 1990, 2015 and 2022

Year/ Land use types	1990		2015		2022	
	Area (Hectares)	Percentage (%)	Area (Hectares)	Percentage (%)	Area (Hectares)	Percentage (%)
Vegetation	10,212	41.91	2,779	11.41	3,236	13.28
Water bodies	416	1.71	298	1.22	228	0.94
Built-up	13,737	56.38	21,228	87.12	20,901	85.78
*No Data	0	0	60	0.25	0	0
Total	**24,365**	**100**	**24,365**	**100**	**24,365**	**100**

*No Data refers to cloud and shadow

Based on the classified map in Figure 3, the uneven distribution of LULC in Kuala Lumpur varied by year. The built-up areas expanded tremendously in almost every part of Kuala Lumpur within 32 years. This pattern was also associated with the loss of vegetation cover as the built-up category took over the green space on a large scale. Moreover, most of the vegetation areas were only concentrated in the west towards the southern part of Kuala Lumpur with a diminished size of the area by 2015. However, the land use pattern in 2022 displayed an exceptional fluctuate trend of vegetation and built-up areas dispersion. From the map roughly, there was a conversion of built-up area into vegetation land from 2015 to 2022. It appeared plausible that the previous barren lands which was categorized as built-up areas had turned into green space for urban agriculture or urban park. Referring to the map, it was apparent that the largest transition of vegetation cover into built-up areas occurred from the west towards the southern end of Kuala Lumpur.

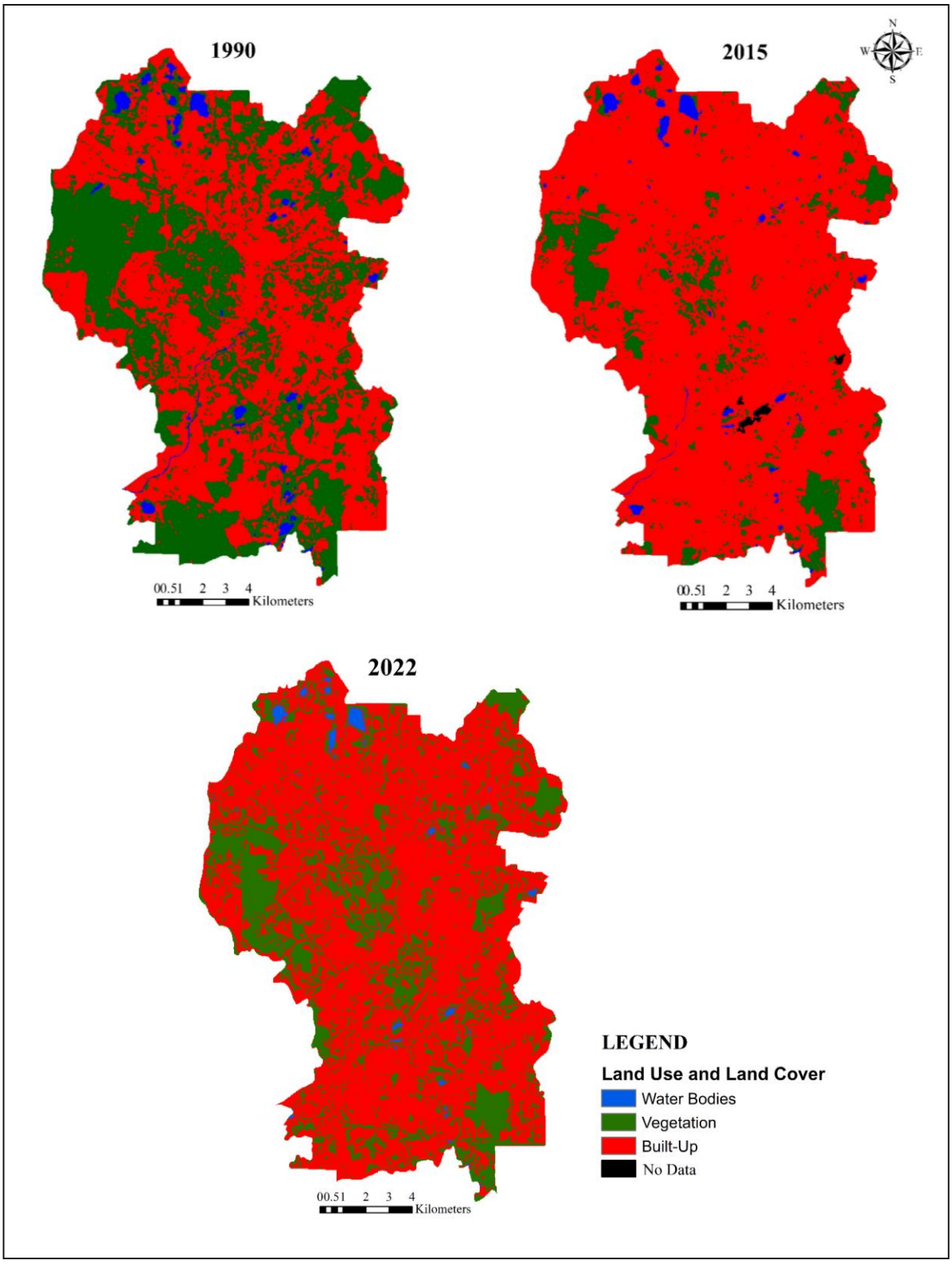

Figure 3. Spatial distribution of land use and land cover in Kuala Lumpur between 1990, 2015 and 2022 through satellite image interpretation

Normalized Difference Vegetation Index (NDVI) and Land Surface Temperature (LST) analysis

Table 3 summarises the NDVI calculation and LST computation for 1990, 2015 and 2022 in Kuala Lumpur. According to the table, the NDVI value for 1990 ranged from -0.523 to 0.712 with an average of 0.299. In 2015, the NDVI values were recorded between -0.209 to 0.584 with an average of 0.216. Whereas the NDVI values for 2022 were between -0.247 to 0.596 with a 0.221 mean value. A massive decline in the NDVI values from 1990 to 2015 and 2022 indicated the gradual absence of vegetation cover in Kuala Lumpur. Meanwhile, the LST values ranged from 20.17 °C to 29.19 °C with a mean of 22.94 °C in 1990. While in 2015, the LST values ranged between 17.35 °C to 30.59 °C with a mean of 25.39 °C. In 2022, the LST values ranged between 13.56 °C to 32.50 °C with an average of 26.22 °C. These statistics indicated that massive development and deforestation accelerated LST mean.

Table 3. Statistics of NDVI and LST value extraction of Kuala Lumpur in 1990, 2015 and 2022

Year	NDVI				LST			
	Min.	Max.	Mean	SD	Min.	Max.	Mean	SD
1990	-0.523	0.712	0.299	0.202	20.17	29.19	22.94	1.21
2015	-0.209	0.584	0.216	0.116	17.35	30.59	25.39	1.51
2022	-0.247	0.596	0.221	0.126	13.56	32.50	26.22	1.89

Min: Minimum, Max: Maximum, SD: Standard deviation

The spatial distribution of NDVI and LST are represented in Figure 4 and Figure 5, respectively. In short, the spatial pattern of LST was closely associated with the distribution of NDVI. Based on the figures, the variations in temperatures were affected by NDVI. The higher the surface temperature, the lower the NDVI value recorded. On the contrary, a higher density of vegetation cover resulted in lower surface temperatures. In 1990, surface temperatures (green-blue colour) of most parts of Kuala Lumpur were lower parallel with the spatial distribution of high NDVI values. However, 2015 and 2022 saw the increase in surface temperatures in many areas as indicated by the yellow-red colour on the map (Figure 4). Hence, less green space cover was observed for NDVI map in 2015 and 2022 (Figure 5). Meanwhile, LST was lower in the high vegetation cover area compared to areas with less vegetation cover.

© 2024, e-ISSN 2682-7727 https://doi.org/10.17576/geo-2024-2001-07

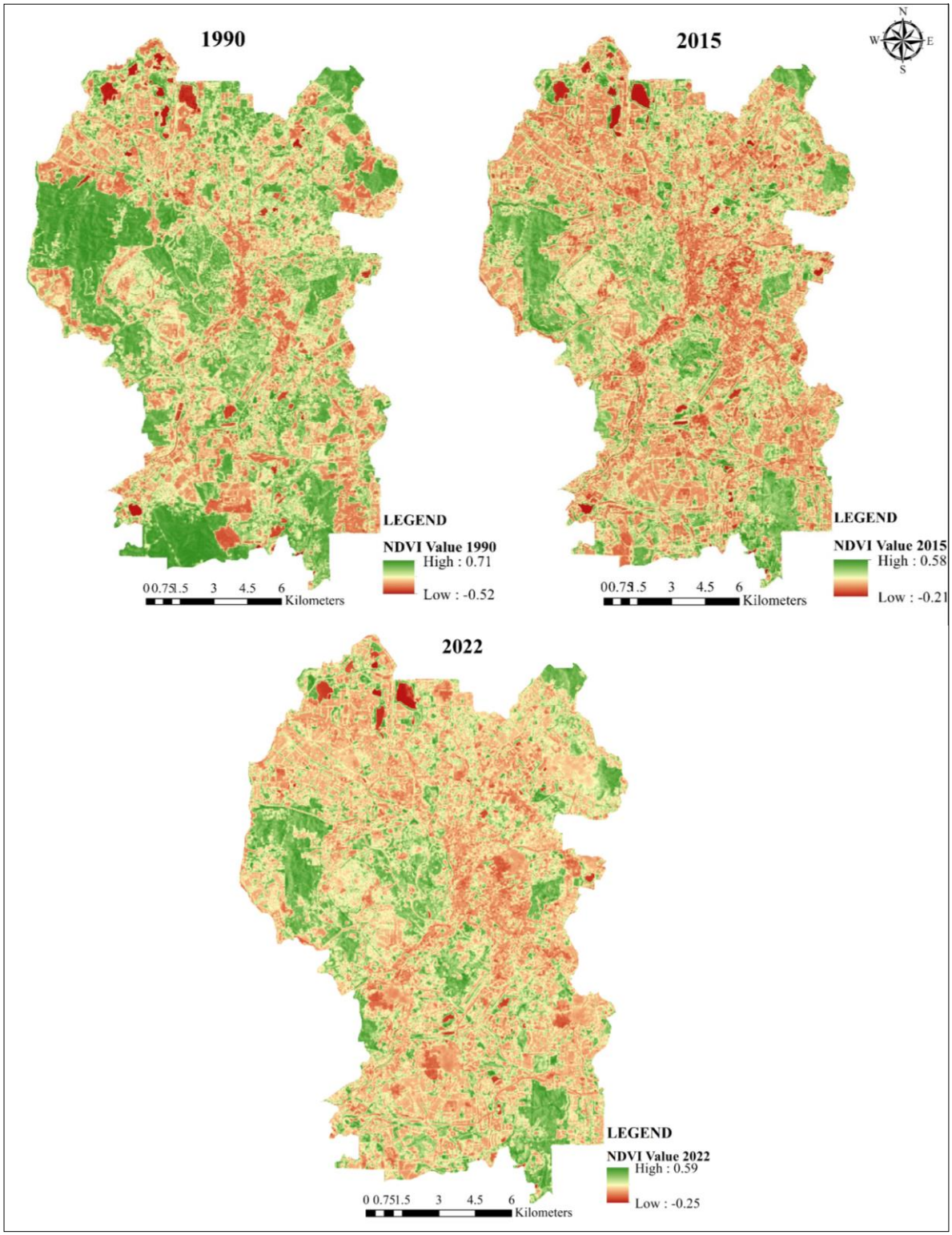

Figure 4. Spatial distribution of NDVI value in Kuala Lumpur between 1990, 2015 and 2022

© 2024, e-ISSN 2682-7727 https://doi.org/10.17576/geo-2024-2001-07

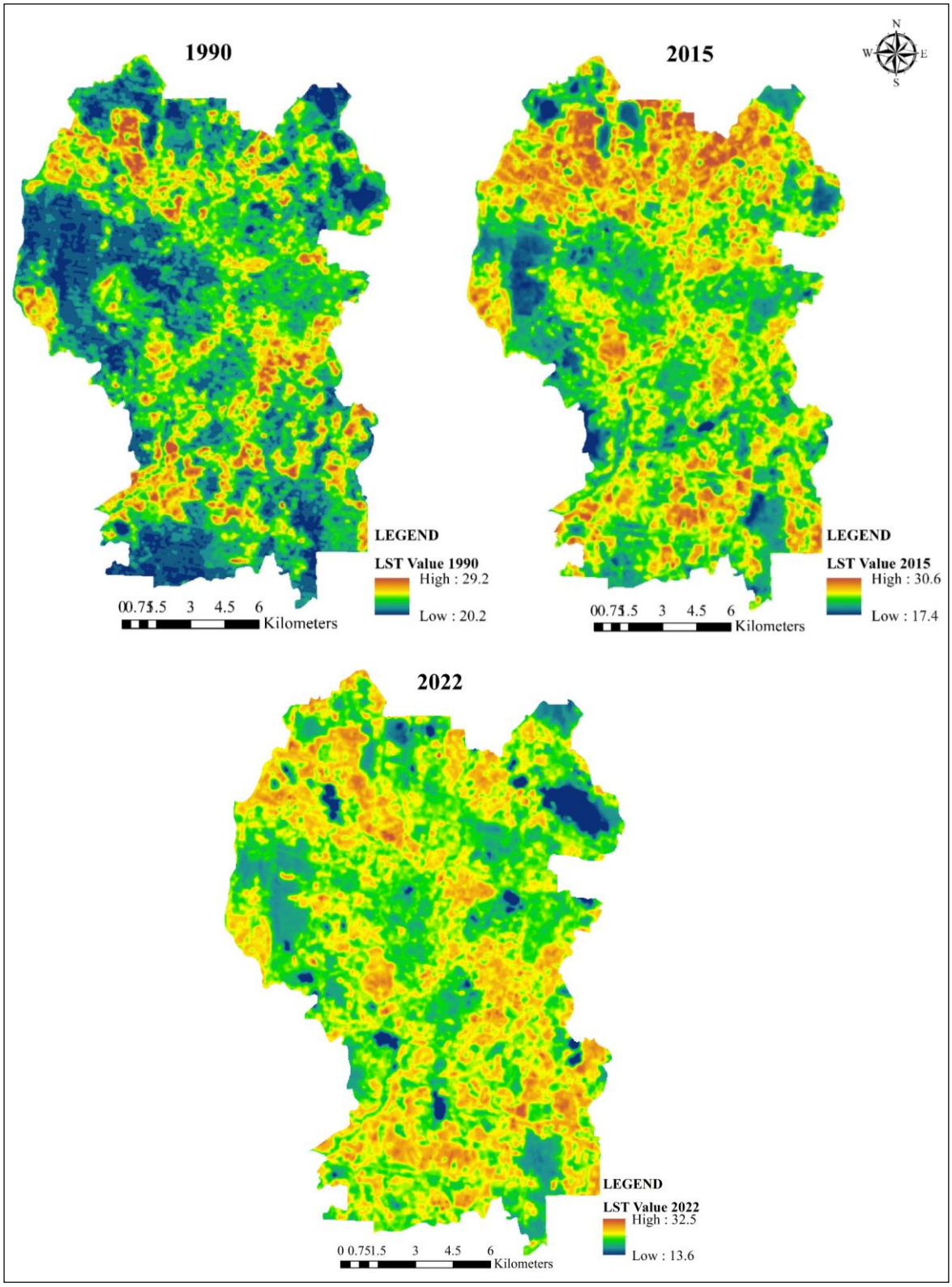

Figure 5. Spatial distribution of LST value in Kuala Lumpur between 1990, 2015 and 2022

Relationship between NDVI and LST based on LULC types

The relationship between NDVI and LST for each LULC was examined using the linear regression correlation. The R-square (R^2) value is the coefficient determination of each regression as indicated in Figure 6, Figure 7, and Figure 8. According to the graph, the relationship between NDVI with LST was negative. The coefficient of determination between LST and NDVI for all the three years where the R^2 values were less than 0.1, with approximately $R^2 = 0.08$ for 1990 and 2015, while R-squared for 2022 was equal to 0.1. These low R-squared results indicated that the correlation between NDVI and LST was inversely correlated because the surface temperature increases with the decrease of NDVI values.

Based on the scatter plots (Figure 6, Figure 7, and Figure 8), the LST of the built-up land was significantly higher compared to the other class types. Whereby water bodies recorded the least due to the low reflectance in NIR and RED spectral bands. In short, the LST was greatly controlled by the characteristics of the surface. This was explained by the results of a p-value of less than 0.05 for all three years which indicated the results were statistically significant at a 0.05 significance level, referring that the land use variation type had an impact on the NDVI and LST value.

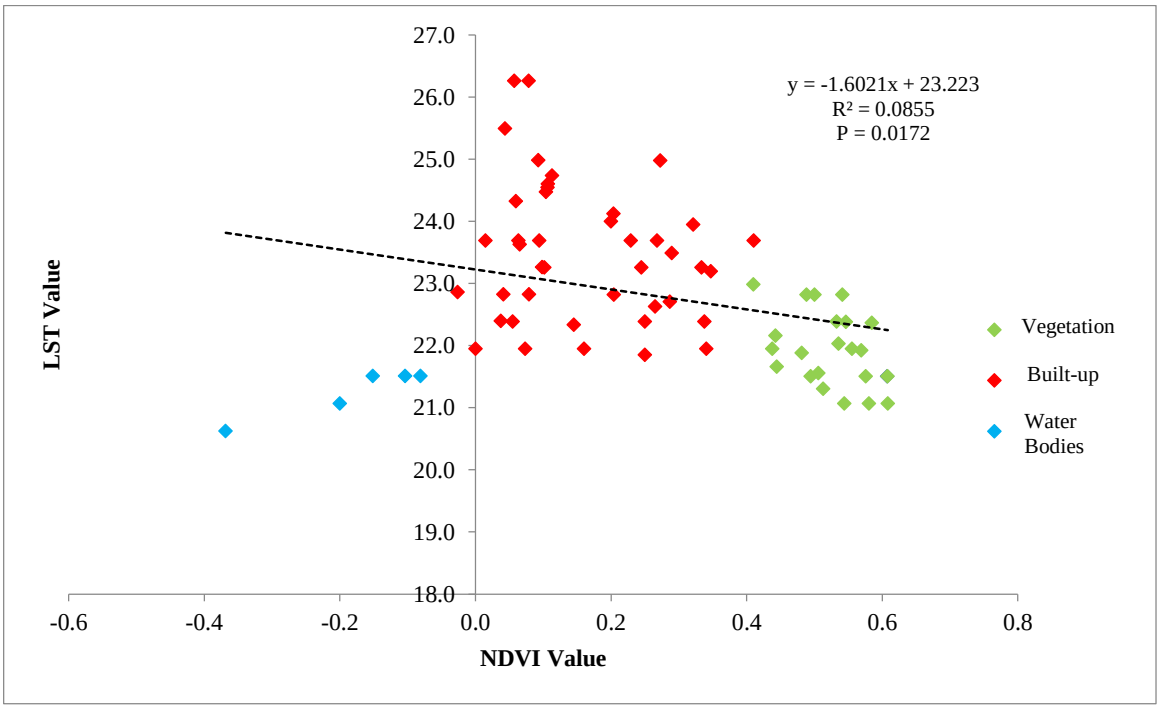

Figure 6. Correlation between NDVI and LST based on LULC types for the study year 1990

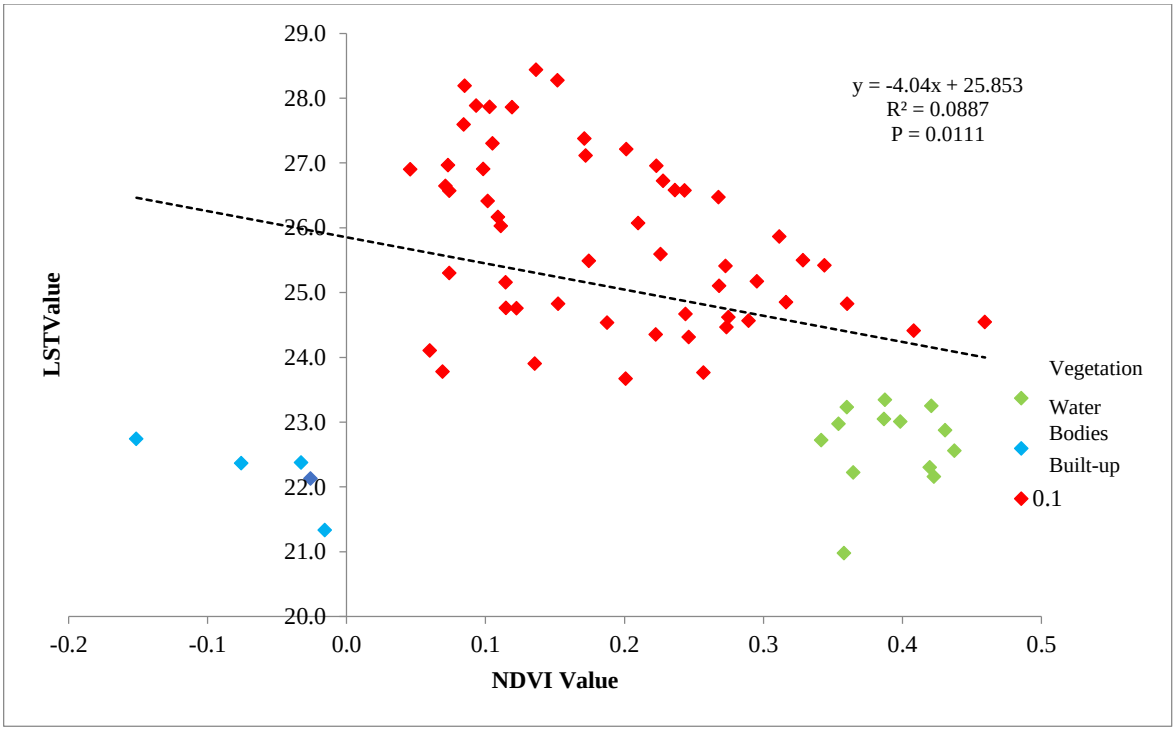

Figure 7. Correlation between NDVI and LST based on LULC types for the study year 2015

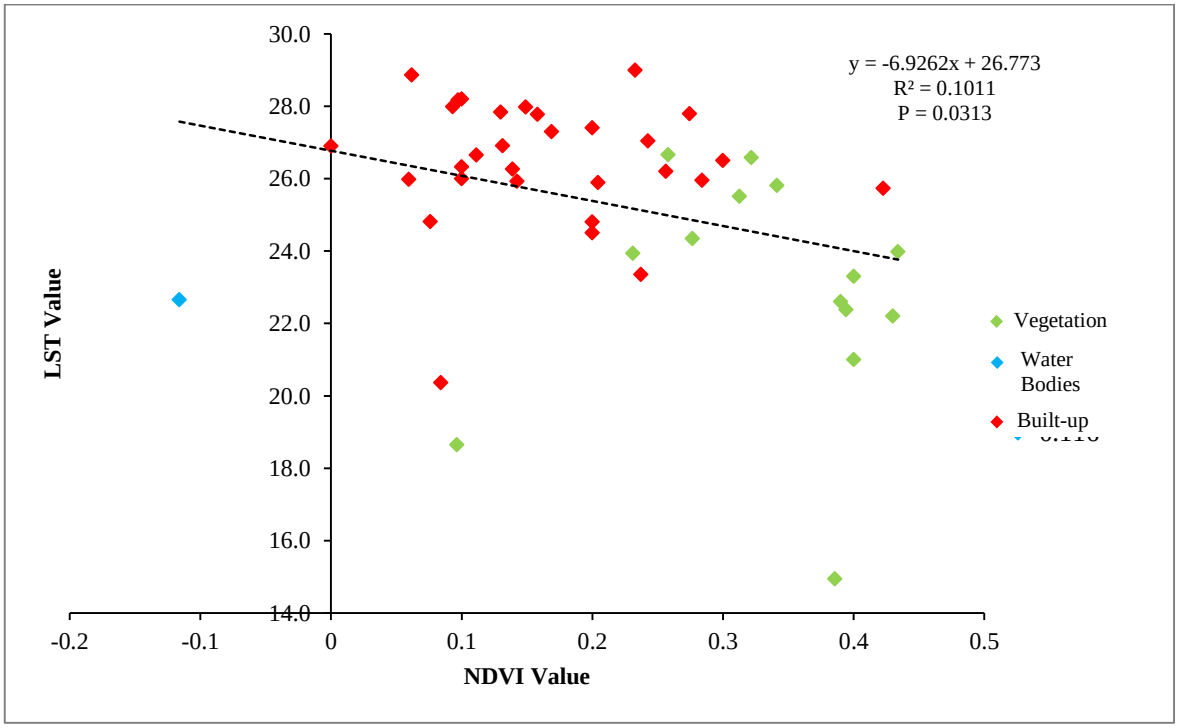

Figure 8. Correlation between NDVI and LST based on LULC types for the study year 2022

Discussion

Since Kuala Lumpur is Malaysia's capital city, this city represents the highly urbanised region of the country. Kuala Lumpur witnessed a rapid developmental phase since the early 1990s as the city encountered significant changes in LULC. Based on the results, the urban development took place in almost every part of Kuala Lumpur starting from the city centre which expanded towards its outskirts within 32 years. Most prominently, the vegetation covers rapidly dwindled, while the built-up lands expanded significantly.

This study revealed a notable reduction of 68% vegetation cover from 1990 to 2022 leaving behind only 13.28% of green cover area within the 32 years. More vegetation cover and water bodies were transformed into high-intensity built-up lands. These alterations resulted in a significant increase in built-up areas by more than 50% within 32 years catering to urban expansion. These observations were in agreement with previous literature, where the urban expansion occurred with the increase in built-up land by converting the green cover and water body areas (Asnawi et al., 2018; Mohd Noor et al., 2013). However, there was an unusual growth of vegetation area in Kuala Lumpur by 2022 compared to previous year of 2015. One of the main focuses in Kuala Lumpur Structure Plan 2040 after the replacement of Kuala Lumpur Structure Plan 2020 to impose greening and beautification) of the city is seen as a determinant in vegetation growth in 2022 (DBKL, 2023). Inherently, the developmental changes of Kuala Lumpur tend to occur at the edge of the existing green space (Nor et al., 2017). Other Asia cities or regions' urban areas expand in the same way with the vegetation loss over the past few decades, such as Cachar region in India (Ashwini & Sil, 2022), Zhejiang Province in China (Wu et al., 2022), Dhaka of Bangladesh (Kafy et al., 2021) and Padang in Indonesia (Ekaputra et al., 2021).

Based on the NDVI values for 1990, 2015 and 2022, the availability of vegetation coverage in Kuala Lumpur decreased intensively. The decreased NDVI value in Kuala Lumpur reflected the deterioration of vegetation health based on the decline of its indicator of green colour. The mean NDVI value which decreased from 0.3 to 0.2 within 32 years was parallel with the loss of vegetation cover in the city. Meanwhile, the mean LST increased between 1990, 2015 and 2022 from 22.9°C jumped to 25.4°C and 26.2°C, respectively. This escalated trend of LST was observed in major parts of Kuala Lumpur. The surface temperature varied with LULC types because different land surface materials project distinct radiation and transmission of heat quantity. Based on the findings, the built-up areas recorded significantly higher surface temperatures than the other LULC categories. These results seemed consistent with other studies which revealed that high-density built-up development with a lack of green cover would raise the LST value in the concentrated urban areas (Saha et al., 2020; Anasuya et al., 2019; Kim et al., 2019; Guo et al. 2012). Lahore of Pakistan (Basheer & Waseem, 2022), Tehran in Iran (Sadeghinia & Sedaghat, 2022), Quang Nam Province and Da Nang City in Vietnam (Nguyen et al., 2022) are among the cities or regions experienced the escalating LST resulting from urbanization.

Generally, the research outcome indicated that LST value was inversely related to NDVI in which parallel with other researchers' findings (Koko et al., 2021; Balew & Korme, 2020; Tafesse & Suryabhagavan, 2019). Contrary, NDVI is highly dependent on LULC (Ismail et al., 2019) that conceivably affects the surface temperature. Where LST decreases with an increase in vegetation cover and increases with an increase in built-up areas (Guha et al., 2018). Beside land surface characteristics, the 2015/2016 El Nino phenomenon was believed to be external factor in fluctuating LST in 2015 which explained the LST rise due to the extreme weather and prolong drought (Kemarau & Eboy, 2023; Yan et al., 2020; Samsuddin et al., 2018).

Consequently, the rising surface temperature is attributed to the phenomenon of Urban Heat Island (UHI) formation which exists in this metropolitan city as disclosed by previous studies (Jumari et al., 2023; Ramakreshnan et al., 2018; Yusuf et al., 2014; Elsayed, 2012). The UHI phenomenon is induced by the urbanisation effects related to the massive and compact urban structures with less vegetation cover and high impermeable surface materials which reduce the cooling effects in the city. There are few cities encountered the same UHI phenomenon because of urban expansion and LST rise, like in Urumqi City in China (Ma et al., 2023), Vienna of Austria (Walder et al., 2022) and Mansoura City in Egypt (Sameh et al., 2022). Hence, it is crucial to take effective measures in combating the adverse effects of urban climate.

In general, government policies such as The National Development Policy 1991-2000, the National Vision Policy 2001-2010, and the Government Transformation Programme 2011-2020 as well as the State Structure Plan and Local Plan play a vital role in influencing national development, including urban development changes in Kuala Lumpur. The government has identified Greater Kuala Lumpur as one of the twelve National Key Economic Areas (NKEAs) which acts as the driver of the economic growth of the country. Consequently, the city has experienced major changes in many socioeconomic aspects which affected its urban physical landscape with more skyscrapers and high-rise buildings filling the view of the city post-2000s. The duration between 1990 until 2022 provided ample time and phases to implement the development planning to cater to the socio-economic needs. The transformation of none-built-up area into built-up land such as the redevelopment project of existing vacant land in Kuala Lumpur affected the urban density (Yin et al., 2022). However, such rapid urban development gave rise to various issues because many natural sources had to be sacrificed. With the rapid developments in Kuala Lumpur, the city started facing the ill effects of excessive urbanisation. The future spatial planning and urban policy of the metropolitan city of Kuala Lumpur will have to endure with perpetual challenges of population rate growth, urban areas instability and monitoring data disorder in urban growth and land-use changes (Boori et al., 2015). Therefore, stakeholders particularly the local authorities need to consider other effective alternatives in compliance with the development regulation to ensure the sustainability of the urban environment.

Conclusion

The time-series data of Landsat imagery utilised to attain the LULC changes, NDVI and LST in Kuala Lumpur over 32 years indicated massive urbanisation of Kuala Lumpur. Based on the findings, Kuala Lumpur had undergone various changes within 32 years since the 1990s. Particularly, the depreciated vegetation cover by more than 65% by 2022 was mostly converted to built-up land. This transformation led to an increase of 3.3 °C LST mean value within 32 years due to less cooling effects in Kuala Lumpur. On the contrary, areas with vegetation cover and water bodies indicated lower LST indicating that LST is negatively correlated with NDVI. In short, the proportion and spatial structure of LULC affect the urban LST. Conjointly, rapid urbanisation in Kuala Lumpur led to the occurrence of regional heating based on the increase in LST value. Therefore, sufficient allocation of vegetation and water body in the city is recommended as a measure to reduce urban heat generation.

Hence, it can be concluded that land-use patterns can directly impact the generation of heat in the urban climate. The identification of NDVI and LST parameters could provide useful information regarding the environmental changes for sustainable urban development and management. This evaluation and interpretation will be helpful in providing knowledge of the dynamic changing of land use implications in Kuala Lumpur to urban and environmental

planners for the monitoring of urbanization and mitigating the effects of rising local temperature. In addition, the integration of remote sensing and GIS application can be considered a powerful tool in monitoring urban changes and the heating phenomenon in urban areas.

There are a few limitations and recommendations for further study, which are:

1. As regards processing time, the algorithm of the maximum likelihood method in classification took less time to perform. However, this conventional algorithm classifier may have limitation on the classification accuracy. Thus, it is recommended to try other classification algorithms for future study.
2. Even though the availability of Landsat data is good, but the Landsat satellite imagery operated in this study has a 30-meter spatial resolution making it difficult to classify land use into more detailed information that produced low classification accuracy. Moreover, its medium image resolution affected the correlation between LST and NDVI. Hence, other data sources such as higher resolution imagery or in situ data can be adopted to obtain more accurate results in the future study.
3. The study further recommends that additional factors like other LULC indices, socioeconomic variables, and other factors could be considered in future studies to produce more sturdy conclusions regarding the surface climate impact study.

References

Al-sharif, A. A. A., & Pradhan, B. (2014). Monitoring and predicting land use change in Tripoli Metropolitan City using an integrated Markov chain and cellular automata models in GIS. *Arabian Journal of Geosciences, 7*(10), 4291-4301.

Alawamy, J. S., Balasundram, S. K., Hanif, A. H. M., & Sung, C. T. B. (2020). Detecting and analyzing land use and land cover changes in the region of Al-Jabal Al-Akhdar, Libya using time-series landsat data from 1985 to 2017. *Sustainability (Switzerland), 12*(11), 4490.

Amanollahi, J., Tzanis, C., Ramli, M. F., & Abdullah, A. M. (2016). Urban heat evolution in a tropical area utilizing landsat imagery. *Atmospheric Research, 167*, 175-182.

Anasuya, B., Swain, D., & Vinoj, V. (2019). Rapid urbanization and associated impacts on land surface temperature changes over Bhubaneswar Urban District, India. *Environmental Monitoring and Assessment, 191*(3), 790.

Angessa, A. T., Lemma, B., & Yeshitela, K. (2019). Land-use and land-cover dynamics and their drivers in the central highlands of Ethiopia with special reference to the Lake Wanchi watershed. *GeoJournal, 86*, 1225-1243.

Asnawi, N. H., Ahmad, P., Choy, L. K., Syahir, M., & Khair, A. A. (2018). Land use and land cover change in Kuala Lumpur using remote sensing and Geographic Information System approach. *Journal of Built Environment, Technology and Engineering, 4*, 206-216.

Aspinall, R.J. (2008). Basic and applied land use science. In Aspinall, R.J., Hill, M.J. (Eds.), *Land use change: Science, policy and management* (pp. 3-11). CRC Press.

Balew, A., & Korme, T. (2020). Monitoring land surface temperature in Bahir Dar city and its surrounding using Landsat images. *The Egyptian Journal of Remote Sensing and Space Science, 23*(3), 371-386.

Basheer, M. A., & Waseem, M. A. (2022). Spatiotemporal analysis of urban growth and land surface temperature: A case study of Lahore, Pakistan. The International Archives of the Photogrammetry, Remote Sensing and Spatial Information Sciences, Volume XLVIII-4/W5, 7th International Conference on Smart Data and Smart Sities (SDSC), 19-21 October, Sydney, Australia.

Bek, M. A., Azmy, N., & Elkafrawy, S. (2018). The effect of unplanned growth of urban areas on heat island phenomena. *Ain Shams Engineering Journal, 9*(4), 3169-3177.

Boori, M.S., Netzband, M., Vozenilek, V., Choudhary, K. (2015). Urbanization analysis through remote sensing and GIS in Kuala Lumpur, Manila and Singapore cities. *Recent Advances in Electrical Engineering, 42*, 99-110.

Buyadi, S., Wan Mohd, W., & Misni, A. (2014). Quantifying green space cooling effects on the urban microclimate using remote sensing and GIS techniques. FIG Congress 2014 Engaging the Challenges, Ehnacing the Relevance.

Cohen, J. (1960). A coefficient of agreement for nominal scales. *Educational and Psychological Measurement, 20*(1), 37-46.

Coll, C., Caselles, V., Valor, E., & Niclòs, R. (2012). Comparison between different sources of atmospheric profiles for land surface temperature retrieval from single channel thermal infrared data. *Remote Sensing of Environment, 117*, 199-210.

Coll, C., Galve, J. M., Sánchez, J. M., & Caselles, V. (2010). Validation of landsat-7/ETM+ thermal-band calibration and atmospheric correction with ground-based measurements. *IEEE Transactions on Geoscience and Remote Sensing, 48*(1), 547-555.

DBKL. (2023). Kuala Lumpur Structure Plan 2040. Dewan Bandaraya Kuala Lumpur.

Dede, M., Pramulatsih, G. P., Widiawaty, M. A., Ramadhan, Y. R., & Ati., A. (2019). Dinamika suhu permukaan dan kerapatan vegetasi di Kota Cirebon. *Jurnal Meteorologi Klimatologi dan Geofisika, 6*(1), 23-31.

Ekaputra, E. G., Stiyanto, E., & Hasanah, N. A. I. (2021, May). Surface temperature across land-use change phenomena in Padang, Indonesia. In *IOP Conference Series: Earth and Environmental* Science, 757(1), 012037.

Elsayed, I. S. M. (2012). A study on the urban heat island of the city of Kuala Lumpur, Malaysia. Journal of King Abdulaziz University - *Meteorology, Environment and Arid Land Agriculture Sciences, 142*(588), 1-27.

Fu, P., & Weng, Q. (2016). A time series analysis of urbanization induced land use and land cover change and its impact on land surface temperature with Landsat imagery. *Remote Sensing of Environment, 175*, 205-214.

Geist, H., Mcconnell, W., Lambin, E. F., Moran, E., Alves, D., Rudel, T. (2006). Causes and trajectories of land-use/cover change. In Lambin, E. F. & Geist, H. (Eds.), *Land-Use and Land-Cover Change: Local Processes and Global Impacts* (pp. 41-70). Springer Science & Business Media.

Guha, S., Govil, H., Dey, A., & Gill, N. (2018). Analytical study of land surface temperature with NDVI and NDBI using Landsat 8 OLI and TIRS data in Florence and Naples city, Italy. *European Journal of Remote Sensing, 51*(1), 667-678.

Guo, Z., Wang, S. D., Cheng, M. M., & Shu, Y. (2012). Assess the effect of different degrees of urbanization on land surface temperature using remote sensing images. *Procedia Environmental Sciences, 13*, 935-942.

Hua, A. K., & Ping, O. W. (2018). The influence of land-use/land-cover changes on land surface temperature: a case study of Kuala Lumpur metropolitan city. *European Journal of Remote Sensing, 51*(1), 1049-1069.

Ismail, N.A., Zin, W.Z.W., Ibrahim, W., Yeun, L.C. (2019). Eight-Day Daytime Land Surface Temperature Pattern over Peninsular Malaysia. *International Journal of Recent Technology and Engineering, 8*(4), 11949–11955.

Imran, H. M., Hossain, A., Islam, A. K. M. S., Rahman, A., Bhuiyan, M. A. E., Paul, S., & Alam, A. (2021). Impact of land cover changes on land surface temperature and human thermal comfort in Dhaka City of Bangladesh. *Earth Systems and Environment, 5*(3), 667-693.

Islam, S., & Ma, M. (2018). Geospatial monitoring of land surface temperature effects on

vegetation dynamics in the southeastern region of Bangladesh from 2001 to 2016. *ISPRS International Journal of Geo-Information*, *7*(12), 486.

Jeevalakshmi, D., Narayana Reddy, S., & Manikiam, B. (2017a). Land surface temperature retrieval from Landsat data using emissivity estimation. *International Journal of Applied Engineering Research*, *12*(20), 9679-9687.

Jeevalakshmi, D., Narayana Reddy, S., & Manikiam, B. (2017b). Land surface temperature retrieval from Landsat data using emissivity estimation. *International Journal of Applied Engineering Research*, *12*(20), 9679-9687.

Jiang, J., & Tian, G. (2010). Analysis of the impact of land use/land cover change on land surface temperature with remote sensing. *Procedia Environmental Sciences*, *2*, 571-575.

Jumari, N. A. S. K., Ahmed, A. N., Huang, Y. F., Ng, J. L., Koo, C. H., Chong, K. L., Sherif, M., & Elshafie, A. (2023). Analysis of urban heat islands with landsat satellite images and GIS in Kuala Lumpur Metropolitan City. *Heliyon*, *9*(8), e18424.

Kafy, A. A., Al Rakib, A., Akter, K. S., Jahir, D. M. A., Sikdar, M. S., Ashrafi, T. J., Mallik, S., & Rahman, M. M. (2021). Assessing and predicting land use/land cover, land surface temperature and urban thermal field variance index using Landsat imagery for Dhaka Metropolitan area. *Environmental Challenges*, *4*, 100192.

Kemarau, R. A., & Eboy, O. V. (2023). Exploring the impact of El Niño–Southern Oscillation (ENSO) on temperature distribution using remote sensing: A case study in Kuching City. *Applied Sciences*, *13*(15), 8861.

Khafid, M. A. (2019). Correlation analysis of the impact of land cover change and ratio vehicles on the dynamic of land surface temperature: Case studies of Cirebon City, Province of West Java. *IOP Conference Series: Earth and Environmental Science*, *399*, 012096.

Killeen, P. G., Mwenifumbo, C.J., & Ford, K. L. (2015). 11.14 – Tools and techniques: Radiometric methods. In Schubert, G. (Second Eds.), *Treatise on Geophysics* (pp.447-524). Elsevier.

Kim, J. I., Jun, M. J., Yeo, C. H., Kwon, K. H., & Hyun, J. Y. (2019). The effects of land use zoning and densification on changes in land surface temperature in Seoul. *Sustainability (Switzerland)*, *11*(24), 7056.

Koko, A. F., Wu, Y., Abubakar, G. A., Alabsi, A. A. N., Hamed, R., & Bello, M. (2021). Thirty years of land use/land cover changes and their impact on urban climate: A study of Kano Metropolis, Nigeria. *Land*, *10*(11), 1106.

Kumar, D., & Shekhar, S. (2015). Statistical analysis of land surface temperature-vegetation indexes relationship through thermal remote sensing. *Ecotoxicology and Environmental Safety*, *121*, 39-44.

Li, Z. L., Tang, B. H., Wu, H., Ren, H., Yan, G., Wan, Z., Trigo, I. F., & Sobrino, J. A. (2013). Satellite-derived land surface temperature: Current status and perspectives. *Remote Sensing of Environment*, *131*, 14-37.

Ma, Y., Mamitimin, Y., Tiemuerbieke, B., Yimaer, R., Huang, M., Chen, H., Tao, T., & Guo, X. (2023). Spatiotemporal characteristics and influencing factors of urban heat island based on geographically weighted regression model: A case study of Urumqi City. *Land*, *12*(11), 2012.

Mallick, J., Kant, Y., Bharath, B. D. (2008). Estimation of land surface temperature over Delhi using Landsat-7 ETM+. *J. Ind. Geophys. Union*, *12*(3), 131-140.

Mashhoodi, B. (2021). Environmental justice and surface temperature: Income, ethnic, gender, and age inequalities. *Sustainable Cities and Society*, *68*, 102810.

Mohd Jaafar, W. S. W., Maulud, K. N. A., Muhmad Kamarulzaman, A. M., Raihan, A., Sah, S. M., Ahmad, A., Maizah Saad, S. N., Mohd Azmi, A. T., Syukri, N. K. A. J., & Khan, W. R. (2020). The influence of deforestation on land surface temperature-A case study of Perak and Kedah, Malaysia. *Forests*, *11*(6), 670.

Mohd Noor, N., Abdullah, A., & Manzahani, M. N. H. (2013). Land cover change detection analysis on urban green area loss using GIS and remote sensing techniques. *Planning Malaysia Journal, 11*(3), 125-138.

Montanaro, M., Gerace, A., Lunsford, A., Reuter, D. (2014). Stray light artifacts in imagery from the Landsat 8 thermal infrared sensor. *Remote Sensing, 6*(11), 10435-10456.

Nguyen, B. Q., Tran, T. N. D., Grodzka-Łukaszewska, M., Sinicyn, G., & Lakshmi, V. (2022). Assessment of urbanization-induced land-use change and its impact on temperature, evaporation, and humidity in central Vietnam. *Water, 14*(21), 3367.

Nor, A. N. M., Corstanje, R., Harris, J. A., & Brewer, T. (2017). Impact of rapid urban expansion on green space structure. *Ecological Indicators, 81*, 274-284.

Pal, S., & Ziaul, S. (2017). Detection of land use and land cover change and land surface temperature in English Bazar urban centre. *Egyptian Journal of Remote Sensing and Space Science, 20*(1), 125-145.

Pamungkas, B. A., Munibah, K., Soma, S. (2019). Land use changes and relation to urban heat island (case study Semarang City, Central Java). *IOP Conference Series: Earth and Environmental Science, 399*, 01206.

Qian, L.-X., Cui, H.-S., & Chang, J. (2006). Impacts of land use and cover change on land surface temperature in the Zhujiang Delta. *Pedosphere, 16*(6), 681-689.

Qin, Z., Karnieli, A., Berliner, P. (2001). A mono-window algorithm for retrieving land surface temperature from Landsat TM data and its application to the Israel-Egypt border region. *International Journal of Remote Sensing, 22*(18), 3719-3746.

Quattrochi, D. A., & Luvall, J. C. (1999). Thermal infrared remote sensing for analysis of landscape ecological processes: Methods and applications. *Landscape Ecology, 14*(6), 577-598.

Rahman, A., Kumar, Y., Fazal, S., & Bhaskaran, S. (2011). Urbanization and quality of urban environment using remote sensing and GIS techniques in East Delhi-India. *Journal of Geographic Information System, 3*(1), 62.

Ramakreshnan, L., Aghamohammadi, N., Fong, C. S., Ghaffarianhoseini, A., Ghaffarianhoseini, A., Wong, L. P., Hassan, N., & Sulaiman, N. M. (2018). A critical review of urban heat island phenomenon in the context of Greater Kuala Lumpur, Malaysia. In *Sustainable Cities and Society, 39*, 99-113.

Rwanga, S. S., & Ndambuki, J. M. (2017). Accuracy assessment of land use/land cover classification using remote sensing and GIS. *International Journal of Geosciences, 8*(4), 611.

Sadeghinia, A., & Sedaghat, M. (2022). Impact of spatiotemporal land use and land cover changes on surface urban heat islands in a semiarid environment. *Időjárás/Quarterly Journal Of The Hungarian Meteorological Service, 126*(4), 425-455.

Saha, P., Bandopadhyay, S., Kumar, C., & Mitra, C. (2020). Multi-approach synergic investigation between land surface temperature and land-use land-cover. *Journal of Earth System Science, 129*(1), 1-21.

Sahana, M., Ahmed, R., & Sajjad, H. (2016). Analyzing land surface temperature distribution in response to land use/land cover change using split window algorithm and spectral radiance model in Sundarban Biosphere Reserve, India. *Modeling Earth Systems and Environment, 2*(2), 81.

Sameh, S., Zarzoura, F., & El-Mewafi, M. (2022). Automated mapping of urban heat island to predict land surface temperature and land use/cover change using machine learning algorithms: Mansoura City. *International Journal of Geoinformatics, 18*(6).

Samsuddin, N. A. C., Khan, M. F., Maulud, K. N. A., Hamid, A. H., Munna, F. T., Ab Rahim, M. A., Latif, M. T., & Akhtaruzzaman, M. (2018). Local and transboundary factors' impacts on trace gases and aerosol during haze episode in 2015 El Niño in

Malaysia. *Science of the total environment*, *630*, 1502-1514.

Sheikhi, A., Kanniah, K. D., & Ho, C. H. (2015). Effect of land cover and green space on land surface temperature of a fast growing economic region in Malaysia. *Earth Resources and Environmental Remote Sensing/GIS Applications VI*, *9644*, 964413.

Sobrino, J. A., Jiménez-Muñoz, J. C., & Paolini, L. (2004). Land surface temperature retrieval from Landsat TM 5. *Remote Sensing of Environment*, *90*(4), 434–440.

Sobrino, J.A., & Raissouni, N. (2000). Toward remote sensing methods for land cover dynamic monitoring: Application to Morocco. *International Journal of Remote Sensing, 21*, 353-366.

Tafesse, B., & Suryabhagavan, K. V. (2019). Systematic modeling of impacts of land-use and land-cover changes on land surface temperature in Adama Zuria District, Ethiopia. *Modeling earth systems and environment*, *5*, 805-817.

Takeuchi, W., Hashim, N., & Thet, K. M. (2010). Application of remote sensing and GIS for monitoring urban heat island in Kuala Lumpur Metropolitan area. Map Asia 2010 and the International Symposium and Exhibition of Geoinformation, Kuala Lumpur.

Tan, K.C., Lim, H. S., MatJafri, M. Z., & Abdullah, K. (2009). Study on land surface temperature based on landsat image over Penang Island, Malaysia. 2009 Sixth International Conference on Computer Graphics, Imaging and Visualization, pp. 525-529.

Tan, Kok Chooi, Lim, H. S., MatJafri, M. Z., & Abdullah, K. (2010). Landsat data to evaluate urban expansion and determine land use/land cover changes in Penang Island, Malaysia. *Environmental Earth Sciences, 60*(7), 1509-1521.

Tang, J., Di, L., Xiao, J., Lu, D., & Zhou, Y. (2017). Impacts of land use and socioeconomic patterns on urban heat island. *International Journal of Remote Sensing, 38*(11), 3445-3465.

Tehrany, M. S., Pradhan, B., & Jebur, M. N. (2013). Remote sensing data reveals eco-environmental changes in urban areas of Klang Valley, Malaysia: Contribution from object based analysis. *Journal of the Indian Society of Remote Sensing, 41*(4), 981-991.

Tran, D. X., Pla, F., Latorre-Carmona, P., Myint, S. W., Caetano, M., & Kieu, H. V. (2017). Characterizing the relationship between land use land cover change and land surface temperature. *ISPRS Journal of Photogrammetry and Remote Sensing, 124*, 119-132.

United Nations, Department of Economic and Social Affairs, Population Division. (2019). *World Urbanization Prospects: The 2018 Revision*. United Nations.

Walder, C., Örs, P. F., & Mahdavi, A. (2022). Land use change impact on urban land surface temperatures: A GIS-supported satellite-based case study. *Acta Polytechnica CTU Proceedings, 38*, 573-578.

Wang, F., Qin, Z., Song, C., Tu, L., Karnieli, A., & Zhao, S. (2015). An improved mono-window algorithm for land surface temperature retrieval from landsat 8 thermal infrared sensor data. *Remote Sensing*, *7*(4), 4268-4289.

Weng, Q., Lu, D., & Schubring, J. (2004). Estimation of land surface temperature-vegetation abundance relationship for urban heat island studies. *Remote Sensing of Environment, 89*(4), 467-483.

Wu, Y., Han, Z., Faisal Koko, A., Zhang, S., Ding, N., & Luo, J. (2022). Analyzing the spatio-temporal dynamics of urban land use expansion and its influencing factors in Zhejiang Province, China. *International Journal of Environmental Research and Public Health*, *19*(24), 16580.

Yan, Y., Mao, K., Shi, J., Piao, S., Shen, X., Dozier, J., Liu, Y., Ren, H. L., & Bao, Q. (2020). Driving forces of land surface temperature anomalous changes in North America in 2002–2018. *Scientific Reports*, *10*(1), 6931.

Yusuf, Y. A., Pradhan, B., & Idrees, M. O. (2014). Spatio-temporal assessment of urban heat island effects in Kuala Lumpur metropolitan city using landsat images. *Journal of the*

Indian Society of Remote Sensing, *42*(4), 829-837.

Zhibin, R., Haifeng, Z., Xingyuan, H., Dan, Z., & Xingyang, Y. (2015). Estimation of the relationship between urban vegetation configuration and land surface temperature with remote sensing. *Journal of the Indian Society of Remote Sensing*, *43*(1), 89-100.

Zhou, X., & Wang, Y. C. (2011). Dynamics of land surface temperature in response to land-use/cover change. *Geographical Research*, *49*(1), 23-36.